DYNAMICS OF EPIDEMIC SPREADING OVER NETWORKS WITH AGENT AWARENESS

A Thesis
Presented to
The Academic Faculty

by

Keith C. Paarporn

In Partial Fulfillment
of the Requirements for the Degree
Master of Science in the
School of Electrical and Computer Engineering

Georgia Institute of Technology
August 2016

DYNAMICS OF EPIDEMIC SPREADING OVER NETWORKS WITH AGENT AWARENESS

Approved by:

Dr. Jeff S. Shamma, Advisor
School of Electrical and Computer Engineering
Georgia Institute of Technology

Dr. Magnus Egerstedt
School of Electrical and Computer Engineering
Georgia Institute of Technology

Dr. Yorai Wardi
School of Electrical and Computer Engineering
Georgia Institute of Technology

Date Approved: July 2016

I would like to thank my family for their continuous support of my graduate studies.

ACKNOWLEDGEMENTS

I would like to thank Professors Jeff Shamma and Joshua Weitz for their guidance and support.

This thesis is supported by ARO grant # W911NF-14-1-0402, and in part by King Abdullah University of Science and Technology (KAUST).

TABLE OF CONTENTS

LIST OF FIGURES

SUMMARY

The research presented in this thesis focuses on a mathematical model of epidemic spreading over complex networks when the population is aware. Individuals receive information about the epidemic from their peers and global broadcasts. They react by reducing their interactions with their neighbors when the epidemic is prevalent and resume normal interactions when it is not. This human behavioral element captures the social distancing actions taken by individuals informed from their social contacts and public service announcements that broadcast advice and recommendations on how to avoid getting sick (e.g. washing hands frequently, avoiding crowded public areas, or staying home from work or school). When the population follows these guidelines, an infectious disease can be prevented from spreading to thousands or even millions of people. The interplay between awareness and social distancing is an effective containment mechanism. The effect of social distancing is an understudied feature in mathematical models of epidemic spreading. The objective of this research is to develop a theoretical understanding of how awareness affects disease spread on a network. Specifically, to what extent can awareness and social distancing mitigate the severity of an epidemic?

CHAPTER I

INTRODUCTION

Epidemics of infectious disease are devastating phenomena occurring throughout history. They not only inflict enormous loss of life, but also significant economic costs to government organizations for treating sick patients, developing vaccines, and preventing the spread of further infections. Useful insights about how disease spreads through a population can be gained by studying mathematical models of epidemics.

1.1 Models of epidemic spread

Mathematical models of epidemic spread have been studied since the 1920's [16]. In the last 20 years, mathematical epidemiology has become a research area of widespread interest, spanning across multiple disciplines and perspectives. This is due to frequent occurences of fast-spreading and deadly epidemics in recent times - for example, HIV/AIDS across the world, the 2002 SARS outbreak in Asia, and recently the Ebola virus in West Africa, just to name a few. Understanding models of epidemic spread can provide insight into how disease propagates through a population and more importantly, what measures can be taken to prevent it from spreading.

The classical models of disease spread are characterized by ODE's (ordinary differential equations) [15], describing the propogation of a virus in a well-mixed population of agents. The population's affliction is described by various states, or compartments. For example, SIS (susceptible-infected-susceptible), SIR (susceptible-infected-recovered), and SEIR (susceptible-exposed-infected-recovered), are among many other variants. In an SIS model, susceptible individuals come into contact with those who are infected, and become infected themselves at a rate proportional to the number of infected people in the population. Individuals who are infected

can heal and become susceptible again at some fixed rate. In these models, coupled ODE equations (one equation for each compartment) describe the interactions and change of populations in each of the different compartments. These types of models represent the population as a continuum of homogeneous and well-mixed individuals. This means that every individual comes into contact with every other individual at the same rate.

A standard result in many of these models establishes a threshold for epidemic persistence. If the disease itself is infectious enough, a constant fraction of the population is always infected. If not, the disease dies out exponentially fast. Specifically, the epidemic persists if $\beta/\delta > 1$ and dies out otherwise, where β is the virus' infection rate and δ is the population's healing rate. The ratio $R_0 = \beta/\delta$ is known as the basic reproductive number, interpreted to be the expected number of secondary infections caused by a single infectious individual over its infectious lifetime. In other words, it is how many agents an infected agent directly infects before it heals. The condition for persistence, $R_0 > 1$, means an infected individual, on average, spreads the disease to more than one other person before it heals.

1.2 Networked models and control

A crucial aspect of realism that is missing is a network structure where each individual can only come into contact with its neighbors. Having the disease dynamics occur over a network (graph) as opposed to a well-mixed population adds spatial and individualistic elements to the model. Along with the explosive research in network science in the last 15 years, disease dynamics on networks is also a growing research topic ([39, 8, 12, 27, 1, 37], among many others). The dynamics are usually modeled as a stochastic process or a mean-field approximation of a stochastic process. Such networked models of epidemics have many other applications not limited to just human diseases - for example, virus propagation in computer networks and the spread

of innovations in social networks.

Just like in the classical ODE models, a standard result in networked epidemic models generalizes the threshold for epidemic persistence. In SIS models, when $\beta/\delta < 1/\lambda_{\max}(A)$, the disease dies out quickly and when $\beta/\delta > 1/\lambda_{\max}(A)$, it persists for a long time. Here, $\lambda_{\max}(A)$ is the maximum eigenvalue of the graph adjacency matrix and $\lambda_{\max}(A)\frac{\beta}{\delta}$ is a generalization of the basic reproductive number R_0 . Thus, the network structure has a role in determining stability properties of the disease spread dynamics. Besides equilibrium properties, another important aspect that arises is the effect network structure has on the spreading dynamics [12, 27, 38, 22].

From a control perspective, one would like to know how to prevent or slow the spread of an ongoing epidemic using limited resources - e.g. a budgeted allocation of vaccines and antidotes over the network [30, 6, 29, 7]. In these models, the allocation decision falls on a single, central authority that knows the entire network structure. This imposes an unrealistic assumption from the perspective of a policymaker. Game theoretic models with self-protection strategies have also been studied where each individual weighs the cost of investing in vaccines against the risk of getting infected [23, 5, 28, 32, 31, 20]. However, these models do not account for social behavior during the course of an epidemic, which can significantly slow spreading without the aid of vaccines.

1.3 Awareness and social distancing

An inherent mechanism in modern society for disease prevention is individual awareness and social distancing, which is the topic of this thesis. People receive information about an ongoing epidemic from their friends or through the news on television, radio, or the internet. The message typically contains advice on how to avoid getting sick (e.g. washing hands frequently, avoiding crowded public areas, etc), or a report of how many people currently are infected.

In the recent 2009 H1N1 Influenza pandemic, people responded to public service announcements by increasing the frequency of washing hands, staying at home when they or loved ones were sick, or avoiding large public gatherings [34]. In the recent Ebola outbreak in West Africa, a combination of quarantining and sanitary burial methods were shown to significantly reduce the rate of virus spread [26]. These precautions effectively limit epidemic spread.

When the population adopts the recommended advice, a disease can be prevented from spreading to thousands or even millions of people. Recent research effort has been devoted to studying the effect of awareness and social distancing in mathematical models of epidemic spread [34, 42, 10, 9, 43]. A review of the existing literature can be found in [40]. The established results show that awareness and social distancing can significantly slow and reduce the severity of an epidemic. Information influences the public's behavior, affecting the course of the epidemic itself, and in turn affecting the public's behavior again. This feedback loop causes the epidemic to coevolve with human social behavior.

1.4 Overview of thesis

This thesis is mainly concerned with SIS epidemic models. Chapter 2 derives basic stability results of a simple SIS ODE model and a variant that incorporates social distancing. Chapter 3 introduces a benchmark networked SIS epidemic Markov chain model. This is then modified to incorporate dynamically distributed awareness and social distancing. The rest of the thesis focuses on the network models. Chapter 4 provides a stochastic comparison analysis between the awareness and benchmark model. Specifically, the benchmark model stochastically dominates the awareness model. The addition of awareness reduces the expectation of any epidemic metric, and the closed-form expression for the reduction is given as a generalized quantity. In Chapter 5, a mean-field approximation of the stochastic model is derived and its

equilibrium properties are studied. In particular, the epidemic threshold is the same for both benchmark and awareness models. Furthermore, the endemic state of the awareness model must be lower than that of the benchmark. Chapter 6 evaluates the effect of social distancing on networks from different random graph families through numerical simulations. Chapter 7 gives concluding remarks.

CHAPTER II

ODE MODELS OF SIS EPIDEMICS

This chapter presents ordinary differential equation (ODE) models of SIS epidemic spread on unaware and aware populations. Stability results are reviewed and are generalized on a network model in later chapters.

2.1 The SIS model

The SIS model is described by the following two-state dynamics,

$$\frac{dS}{dt} = \delta I - \frac{\beta SI}{N} \quad \text{Susceptible population} \tag{1}$$

$$\frac{dI}{dt} = \frac{\beta SI}{N} - \delta I \quad \text{Infected population} \tag{2}$$

where $\beta > 0$ is the infection rate of the disease, $\delta > 0$ is the healing rate, and $N > 0$ is the size of the population. One can interpret this model as having a continuum of agents of mass N, where the population is homogeneous and well-mixed. Here, we assume that $S(0) + I(0) = N$ with $0 \leq S(0), I(0) \leq N$. The fact that $\frac{d}{dt}(S + I) = 0$ ensures $S(t) + I(t) = N$ with $S(t), I(t) \geq 0 \ \forall t$, so the total population is kept constant and the dynamics can be described by just one state variable. The infected population heals to become susceptible at a rate proportional to its level. The susceptible population becomes infected by interacting with the infected population (see Figure 1). In phase space, the point $(S^*, I^*) = (N, 0)$ (all-susceptible state) is always an equilibrium point. The Jacobian matrix is

$$J = \begin{bmatrix} -\frac{\beta I}{N} & -\frac{\beta S}{N} + \delta \\ \frac{\beta I}{N} & \frac{\beta S}{N} - \delta \end{bmatrix} \tag{3}$$

Stability analysis shows it is stable if $R_0 = \beta/\delta < 1$ (recall R_0 is the basic reproductive number). To see this, rewrite $\frac{dI}{dt} = I\left(\frac{\beta S}{N} - \delta\right)$. The quantity in the parentheses is

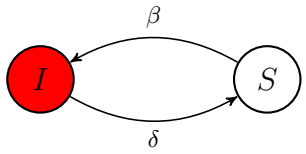

Figure 1: SIS dynamics state transition diagram

always strictly negative, and hence $I(t) \to 0$. It is unstable if $R_0 > 1$. When (S^*, I^*) is unstable, there exists another equilibrium point $(\hat{S}, \hat{I}) = (\frac{\delta}{\beta}N, N(1 - \frac{\delta}{\beta}))$ which is stable. This equilibrium is known in the epidemiology literature as the endemic state, where a fraction of the population is always infected. In this scenario, the disease is infectious enough to sustain itself within the population.

We already see that a simple mathematical model of epidemic spreading gives rise to a rich set of dynamics. It turns out this model can be solved analytically.

2.2 Exact solution to the SIS ODE

One can derive the closed-form solution to the set of ODE's in the previous section. Since $S(t) = N - I(t)$, it amounts to solving a single variable ODE,

$$\frac{dI}{dt} = I\left(\beta(1 - \frac{I}{N}) - \delta\right). \tag{4}$$

We rearrange by dividing:

$$\frac{dI/dt}{I\left(\beta(1 - \frac{I}{N}) - \delta\right)} = 1 \tag{5}$$

Let $c_N := N(\delta/\beta - 1)$. Using a partial fraction decomposition on the left-hand side, we obtain

$$\left(\frac{dI/dt}{I} - \frac{dI/dt}{I + c_N}\right) = -\frac{\beta}{N}c_N \tag{6}$$

Integrating from 0 to t with respect to the time variable, we get

$$[\log(I(t)) - \log(I(0)) - \log(I(t) + c_N) + \log(I(0) + c_N)] = -\frac{\beta}{N}c_N t \tag{7}$$

Taking the exponential,

$$\frac{I(t)}{I(0)} \times \frac{I(0) + c_N}{I(t) + c_N} = e^{(\beta - \delta)t} \tag{8}$$

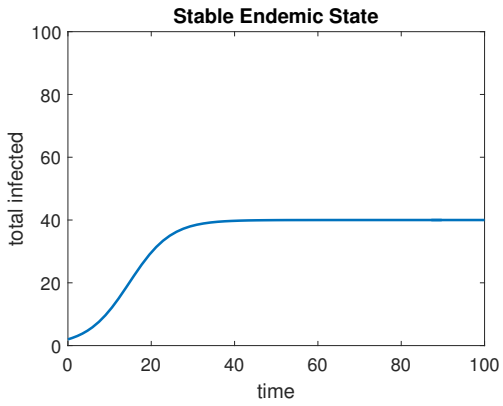

(a) $I(t)$ when $\beta > \delta$. Here, $\beta = 0.5, \delta = 0.3, N = 100, I(0) = 2$.

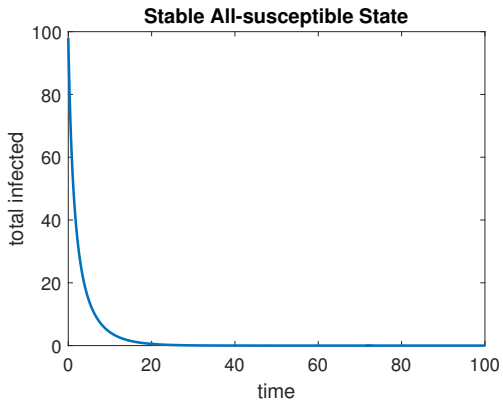

(b) $I(t)$ when $\beta < \delta$. Here, $\beta = 0.5, \delta = 0.7, N = 100, I(0) = 98$.

Figure 2: Solution to SIS epidemic ODE

Solving for $I(t)$, we obtain

$$I(t) = \hat{I} \times \frac{I(0)e^{(\beta-\delta)t}}{I(0)\left(e^{(\beta-\delta)t} - 1\right) + \hat{I}} \tag{9}$$

where we recall that $\hat{I} = N(1 - \frac{\delta}{\beta})$.

The solution (9) is consistent with the stability analysis of the previous section (see Figure 2). When $\beta < \delta$, the numerator vanishes for large t, so $I(t) \to 0$. When $\beta > \delta$, the exponential terms in the numerator and denominator dominate. Thus, $I(t) \to N(1 - \delta/\beta) = \hat{I}$. This holds for $0 < I(0) \leq N$.

2.3 An SIS model with social distancing

The SIS ODE's (1) and (2) describe the physical process of disease spreading in an unaware population. Here, we introduce a modified version of equations (1) and (2) to model the population's awareness and social distancing actions:

$$\frac{dS}{dt} = \delta I - \frac{\beta(1 - \frac{I}{N})SI}{N} \quad \text{Susceptible population} \tag{10}$$

$$\frac{dI}{dt} = \frac{\beta(1 - \frac{I}{N})SI}{N} - \delta I \quad \text{Infected population} \tag{11}$$

The term $\beta(1 - \frac{I}{N})$ is the reduction in contact with the infected population due to social distancing taken by the agents in the population. It is a function of the total

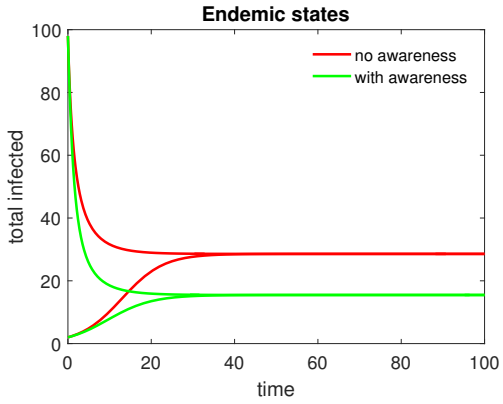

(a) $I(t)$ when $\beta > \delta$ for $I(0) = 2, 98$. $\beta = 0.5, \delta = 0.3, N = 100$.

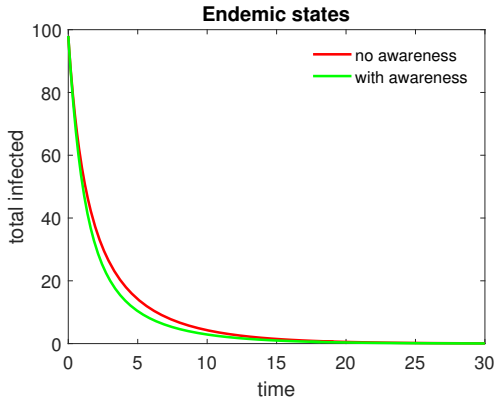

(b) $I(t)$ when $\beta < \delta$. $\beta = 0.5, \delta = 0.3, N = 100, I(0) = 98$.

Figure 3: Comparison of $I(t)$ between models with and without awareness.

number of infected individuals in the population. Hence, one can think of I/N as an agent's awareness, i.e. an agent knows the fraction of the population that is infected. Here, the distancing is linear in I, although one could easily make it any decreasing function of I, e.g. $\beta(1 - \frac{I}{N})^k$ with $k = 1, 2, \ldots$. Again, The ODE's can be expressed as a single ODE in one variable,

$$\frac{dI}{dt} = I\left(\frac{\beta(N-I)^2}{N^2} - \delta\right). \tag{12}$$

There are two equilibria of equation (12) - the all-susceptible state $I^* = 0$ and an endemic state $\hat{I} = N(1 - \sqrt{\delta/\beta})$, feasible only when $\delta < \beta$. We can rewrite (12) as

$$\frac{dI}{dt} = I\left(\beta\frac{S^2}{N^2} - \delta\right). \tag{13}$$

Since $S \leq N$, the term in parenthesis is always negative if $\delta > \beta$. Thus, for any $0 < I(0) \leq N$, $I(t) \to 0$. When $\delta < \beta$, we look at two cases. When $S(0) < N\sqrt{\delta/\beta}$ (or $I(0) > \hat{I}$), the term in the parentheses is negative. When $S(0) > N\sqrt{\delta/\beta}$ (or $I(0) < \hat{I}$), the term is positive. Thus, $I(t) \to \hat{I}$ whenever $0 < I(0) \leq N$.

Furthermore, one can conclude that if $I(t)$ is a solution to (2) and $I_a(t)$ is a solution to (11) on $[0, \infty)$, then $I(t) \geq I_a(t)$ whenever $I(0) \geq I_a(0)$. Indeed, $S/N \geq (S/N)^2$ for any $0 \leq S \leq N$, and hence the right-hand side of (2) is greater or equal to

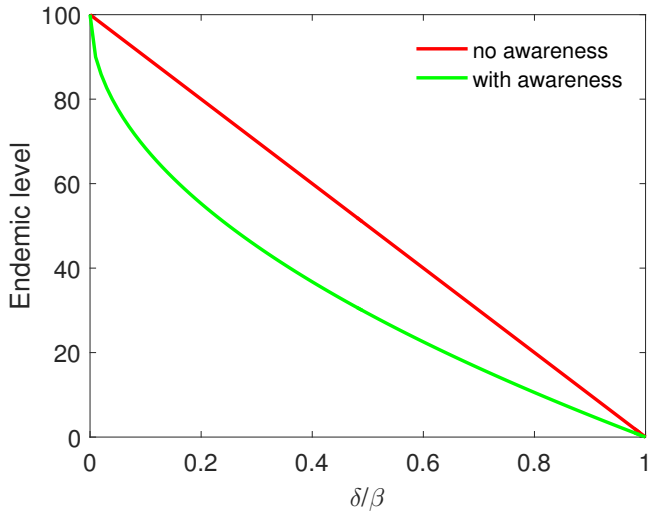

Figure 4: Long-run total infected $\hat{I}$ as a function of δ/β in the endemic regime $\delta/\beta < 1$.

the right-hand side of (11). We get the result by applying the Comparison Lemma (Lemma 3.4, [17]). Hence, the total infected in an aware population is bounded above by the total infected in an unaware population.

The addition of social distancing lowers the overall endemic state, but does not change its stability properties. That is, social distancing does not affect the threshold ($\delta/\beta < 1$) for epidemic persistence.

2.4 Summary

In this chapter we studied a basic SIS process modeled as an ODE. When the disease is infectious enough, a constant fraction of the population remains infected in the long run. Otherwise, the disease will always eradicate exponentially fast. The ODE was then modified to incorporate an element of social distancing, in which the same equilibrium conclusions are drawn. We will see in Chapter 5 that the same conclusions still hold when a stochastic version of the model is adapted to an arbitrary network.

CHAPTER III

NETWORK MODELS OF SIS EPIDEMICS

3.1 The benchmark SIS model

Here, a standard model of epidemic spreading over a finite static network of n agents is introduced (studied in [39],[2], and Section 5 of [1]), which we will refer to as the benchmark model. Consider the set of nodes $\mathcal{N} = \{1, \ldots, n\}$ interconnected by a set of edges $\mathcal{E}$. Epidemic spread occurs in discrete time steps $t = 0, 1, \ldots$ over the undirected graph $\mathcal{G}_C = (\mathcal{N}, \mathcal{E})$, whose $n \times n$ adjacency matrix is defined for any $i, j \in \mathcal{N}$, as $[A_C]_{ij} = 1$ if $(i, j) \in \mathcal{E}$ and 0 otherwise. The graph $\mathcal{G}_C$ will be refered to as the contact network. An agent $i \in \mathcal{N}$ is either susceptible to the disease or infected by it. The epidemic states are defined as $\Omega = \{0, 1\}^n$. For any $s \in \Omega$ and $i \in \mathcal{N}$, either $s_i = 0$, meaning agent i is susceptible, or $s_i = 1$, meaning it is infected. Susceptible agents can contract the disease from neighboring agents in the contact network. When agent i is susceptible in the epidemic state is $s \in \Omega$ ($s_i = 0$), its probability of getting infected in the next time step due to an interaction with its neighbor $j \in \mathcal{N}_i^C$ is given by βs_j where $\beta \in (0, 1)$ is the transmission probability of the disease. Hence, an individual can only contract the disease from an infected neighbor. Agent i interacts with each of its neighbors independently. Therefore, i's probability of not becoming infected in the next time step is

$$p_{00}^i(s) = \prod_{j \in \mathcal{N}_i^C} (1 - \beta s_j) \tag{14}$$

Consequently, its probability of getting infected is

$$p_{01}^i(s) = 1 - p_{00}^i(s) = 1 - \prod_{j \in \mathcal{N}_i^C} (1 - \beta s_j) \tag{15}$$

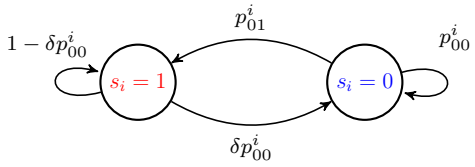

Figure 5: SIS dynamics state transition diagram

When agent i is infected in state $s \in \Omega$ ($s_i = 1$), it becomes susceptible in the next time step with probability $\delta p^i_{00}(s)$, where $\delta \in (0,1)$ is the healing probability of the disease. Thus, for an infected node to become susceptible, it must heal and not get re-infected by its neighbors. Node i's transition probabilities are illustrated in Figure 5 and summarized by $\mathbb{P}_i : \Omega \times \{0,1\} \to [0,1]$ defined by

$$\text{If } s_i = 0, \begin{cases} \mathbb{P}_i(s,0) & = p^i_{00}(s) \\ \mathbb{P}_i(s,1) & = p^i_{01}(s) \end{cases} \tag{16}$$

$$\text{If } s_i = 1, \begin{cases} \mathbb{P}_i(s,0) & = \delta p^i_{00}(s) \\ \mathbb{P}_i(s,1) & = 1 - \delta p^i_{00}(s) \end{cases} \tag{17}$$

For each $i \in \mathcal{N}$ and $s \in \Omega$, the $\mathbb{P}_i$ define the benchmark SIS Markov chain over Ω by the $2^n \times 2^n$ transition matrix K with elements

$$K(s,s') \triangleq \prod_{i=1}^{n} \mathbb{P}_i(s, s'_i), \ \forall s, s' \in \Omega \tag{18}$$

This chain has one absorbing state, the all-susceptible state $\mathbf{o} \triangleq \{0\}^n$.

3.2 The awareness SIS model

We modify the benchmark model to take into account the agents' awareness of the current epidemic state. The information agent i receives comes from two sources: the proportion of infected neighbors in its local social network and a global broadcast of the proportion of infected nodes in the entire network. The social network is a graph $\mathcal{G}_I = (\mathcal{N}, \mathcal{E}_I)$ with the same nodes as $\mathcal{G}_C$ but with different edges, representing the

nodes' social communication links. The set of i's neighbors in $\mathcal{G}_I$ is written $\mathcal{N}_i^I$. The information is given by

$$\mu_i(s) \triangleq \frac{\alpha}{|\mathcal{N}_i^I|} \sum_{j \in \mathcal{N}_i^I} s_j + \frac{1-\alpha}{n} \sum_{j=1}^{n} s_j \ , \forall s \in \Omega \tag{19}$$

where $\alpha \in [0,1]$ is a parameter that governs the trust nodes place in information from their social contacts. Consequently, node i reduces its interactions with its physical neighbors through the social distancing action

$$a_i(s) \triangleq 1 - \mu_i(s), \tag{20}$$

which reduces its susceptible-to-infected probability (15) to

$$p_{01,d}^i(s) \triangleq 1 - \prod_{j \in \mathcal{N}_i^C} (1 - \beta a_i(s) s_j). \tag{21}$$

We similarly define $p_{00,d}^i(s) \triangleq 1 - p_{01,d}^i(s)$. An infected agent's probability of recovering becomes $\delta p_{00,d}^i(s)$. Note for all $s \in \Omega$, $p_{01,d}^i(s) \leq p_{01}^i(s)$. Combined with the social distancing behaviors a_i, the local awareness spread dynamics in (19) make the effect of user behavior on its infection probability endogenous to the benchmark chain model through a negative feedback loop. We define the $\mathbb{P}_i^d$ analogously to (16) and (17):

$$\text{If } s_i = 0, \begin{cases} \mathbb{P}_i^d(s,0) & = p_{00,d}^i(s) \\ \mathbb{P}_i^d(s,1) & = p_{01,d}^i(s) \end{cases} \tag{22}$$

$$\text{If } s_i = 1, \begin{cases} \mathbb{P}_i^d(s,0) & = \delta p_{00,d}^i(s) \\ \mathbb{P}_i^d(s,1) & = 1 - \delta p_{00,d}^i(s) \end{cases} \tag{23}$$

Thus, the $\mathbb{P}_i^d$ define the distancing Markov chain over Ω by the transition matrix K_d with elements

$$K_d(s,s') \triangleq \prod_{i=1}^{n} \mathbb{P}_i^d(s, s_i'), \ \forall s, s' \in \Omega \tag{24}$$

whose unique absorbing state is also $\mathbf{o}$, the all-susceptible state. The feedback loop between the epidemic state and agent awareness is illustrated in Figure 6. An instance of sample trajectories is shown in Figure 7.

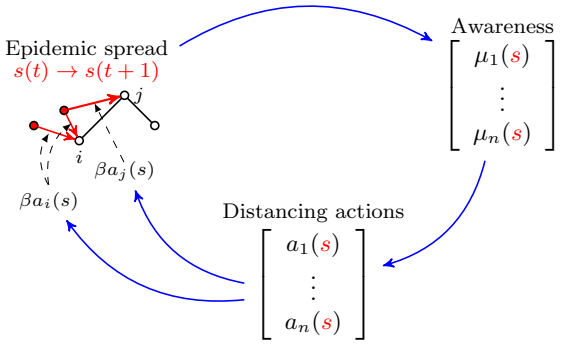

Figure 6: System-level diagram

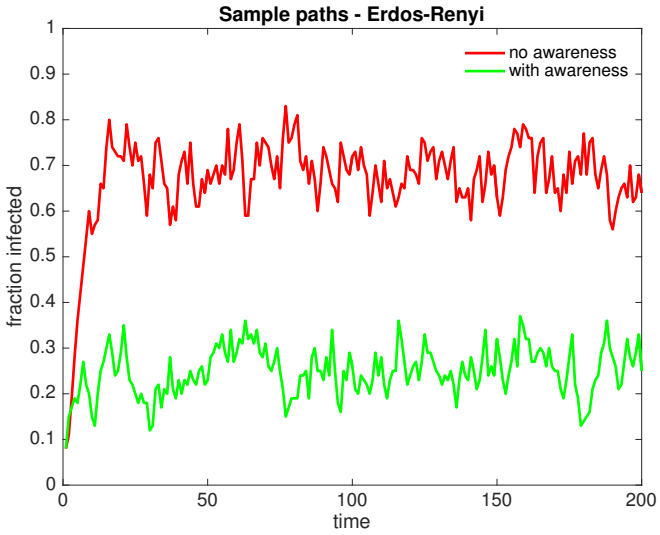

Figure 7: A pair of sample paths generated from the Markov chain models. Here, $\beta = 0.1, \delta = 0.5, \alpha = 1$, and $\mathcal{G}_I = \mathcal{G}_C$. Performed on a 100 node Erdős-Renyi network with parameter $p = 0.1$.

The awareness model captures the different ways an agent may receive information about an ongoing epidemic from the media. Large media corporations and public health institutions such as the Centers for Disease Control and Prevention (CDC) and the World Health Organization (WHO) often report an estimated total number of people infected nationwide or globally at a given time, and this information is disseminated amongst the population. Information is also exchanged through one's personalized social links, which can range beyond a person's geographic location.

It is important to note that since the all-susceptible state is the unique absorbing state for both benchmark and awareness chains, and it is accessible from all other states, the chains must eventually absorb in finite time with probability one. This reveals the long-run equilibrium properties, but says nothing about what happens in the medium-run, before the disease dies out. The expected absorption time grows exponentially with the size of the network. Thus, one must wait an unrealistically long time for the epidemic to die out.

3.3 Summary

This chapter presented a networked SIS model with and without awareness. The benchmark model has previously been studied in the literature. In our awareness model, each agent receives personalized information from its social network and a global broadcast. This causes them to reduce their interaction level with their physical neighbors, making them less likely to become infected.

CHAPTER IV

STOCHASTIC COMPARISON ANALYSIS

This chapter presents a stochastic comparison analysis between the benchmark and awareness Markov chain models via a monotone coupling framework. The analysis shows awareness reduces the expectation of any epidemic cost metric (e.g. time to extinction, total infected over time, etc) and the reduction can be given as a closed-form expression. First, relevant definitions and examples on monotone couplings are given. For a full reference on monotone coupling, see Ch 4 of [19].

4.1 Monotone couplings

Consider a general countable space X. A partially ordered set $(X, \preceq_X)$ is the set X together with a relation $\preceq_X$ among its elements which satisfies for all x, y, and $z \in X$,

- $x \preceq_X x$
- If $x \preceq_X y$ and $y \preceq_X z$, then $x \preceq_X z$
- If $x \preceq_X y$ and $y \preceq_X x$, then $x = y$.

Definition 1. Let p_1, p_2 be probability measures on a measurable space $(X, \mathcal{F})$ and suppose $(X, \preceq_X)$ is a partially ordered set. A *monotone coupling* of p_1, p_2 is a probability measure p on $(X^2, \mathcal{F}^2)$ such that for all $x', y' \in X$,

$$\sum_{x \preceq_X y'} p(x, y') = p_2(y') \text{ and } \sum_{y \succeq_X x'} p(x', y) = p_1(x'). \tag{25}$$

Thus, for any $x, y \in X$ s.t $x \not\preceq_X y$, $p(x, y) = 0$. A monotone coupling p can be thought of as a joint distribution on two possibly independent random variables whose distributions are given by p_1, p_2, where one of them "dominates" the other in terms of a partial ordering.

Example 1. Consider two biased coins A and B where the biases $q_A, q_B < 1$ for landing heads satisfy $q_A < q_B$. The independent distributions are given by $p_X(0) = 1 - q_X, p_X(1) = q_X$ for $X \in \{A, B\}$. The coupling is a joint distribution assigned to the pair of coin flips to ensure the q_A coin can never land heads with the q_B coin landing tails, while the marginal coin flip probabilities remain the same. Also, define $p_{AB} : \{0,1\}^2 \to [0,1]$ by

$$\begin{cases} p_{AB}(0,0) &= 1 - q_B \\ p_{AB}(0,1) &= q_B - q_A \\ p_{AB}(1,0) &= 0 \\ p_{AB}(1,1) &= q_A \end{cases} \tag{26}$$

Checking (25), the marginals are such that $\sum_{b \geq 1} p_{AB}(1,b) = q_A$, $\sum_{a \leq 1} p_{AB}(a,1) = q_B$ and $\sum_{b \geq 0} p_{AB}(0,b) = 1 - q_A$, $\sum_{a \leq 0} p_{AB}(a,0) = 1 - q_B$. Thus, p_{AB} is a monotone coupling of p_A, p_B.

A function $Z : X \to \mathbb{R}$ is *increasing in* X if whenever $x \preceq_X y$, $Z(x) \leq Z(y)$. The next result characterizes the difference in expectations of increasing random variables between the marginals of a monotone coupling.

Proposition 1. Keeping the notation of Definition 1, suppose p is a monotone coupling of p_1, p_2. If a random variable $Z : X \to \mathbb{Z}_+$ is increasing in X, then

$$\mathbb{E}_{p_2}(Z) - \mathbb{E}_{p_1}(Z) = \sum_{\tau=0}^{\infty} p(Z_\tau^c, Z_\tau) \tag{27}$$

where $Z_\tau = \{x : Z(x) > \tau\}$.

Proof. Consider the following quantities:

$$\begin{aligned} p(Z_\tau, Z_\tau) &= \sum_{x \in Z_\tau} \sum_{y \in Z_\tau} p(x,y) \\ &= \sum_{x \in Z_\tau} \sum_{y \succeq_X x} p(x,y) = p_1(Z_\tau) \end{aligned} \tag{28}$$

$$p(X, Z_\tau) = p_2(Z_\tau) \tag{29}$$

The second sum over $\{y \in Z_\tau\}$ can be replaced with $\{y \succeq_X x\}$ in (28) because 1) for any $x \in Z_\tau$, we have $\{y : y \succeq_X x\} \subset Z_\tau$; and 2) since p is a monotone coupling, for any $y \in Z_\tau$ s.t. $y \not\succeq_X x$, $p(x, y) = 0$. The last equality of (28) follows from (25). Since $(X, Z_\tau) \supset (Z_\tau, Z_\tau)$ we can write

$$\begin{aligned} p_2(Z_\tau) - p_1(Z_\tau) &= p(X, Z_\tau) - p(Z_\tau, Z_\tau) \\ &= p((X, Z_\tau) \backslash (Z_\tau, Z_\tau)) \\ &= p(Z_\tau^c, Z_\tau) \end{aligned}$$

Equation (27) immediately follows. ■

Example 2. Consider the biased coins of Example 1. This example can be extended to sequences of $m \geq 2$ flips, $\{0, 1\}^m$ with the partial order $x \preceq y$ if $x_i \leq y_i$, $i = 1, \ldots, m$, for $x, y \in \{0, 1\}^m$. Define

$$\overline{p}_X(x) = \prod_{k=1}^{m} p_X(x_k), \ X \in \{A, B\} \tag{30}$$

$$\overline{p}_{AB}(x, y) = \prod_{k=1}^{m} p_{AB}(x_k, y_k). \tag{31}$$

Then $\overline{p}_{AB}$ is a monotone coupling of $\overline{p}_A, \overline{p}_B$. For $x \in \{0, 1\}^m$, let $Z(x) = \sum_{i=1}^m x_i$ be the random variable of the number of heads for any given toss sequence. Then Z is increasing in $\{0, 1\}^m$. By Proposition 1,

$$\mathbb{E}_{\overline{p}_B}(Z) - \mathbb{E}_{\overline{p}_A}(Z) = \sum_{\tau=0}^{m} \overline{p}_{AB}(Z_\tau^c, Z_\tau). \tag{32}$$

Of course, one could trivially compute the LHS above as $m(q_B - q_A)$ since the distribution of Z is Bernoulli. However, Proposition 1 generalizes the difference for any increasing $\mathbb{Z}_+$-valued random variable over a partially ordered set.

The notion of stochastic domination is a natural concept that arises in monotone couplings.

Definition 2. An *upper set* $\mathcal{I}$ is a non-empty subset of $(X, \preceq_X)$ that satisfies the following property: if $x \in \mathcal{I}$ and $y \succeq_X x$, then $y \in \mathcal{I}$. Let p_1, p_2 be two probability measures on $(X, \mathcal{F})$. Then p_2 *stochastically dominates* p_1, written as $p_2 \succeq p_1$, if for any upper set $\mathcal{I} \subset X$, $p_1(\mathcal{I}) \leq p_2(\mathcal{I})$.

The comparison between benchmark and distancing chains falls into the framework of the above analysis.

4.2 Comparison over sample paths

Our main result provides a construction of a monotone coupling between the benchmark and distancing probability distributions on sample paths.

Definition 3. A *sample path* is a sequence $g = \{g^t\}_{t \in \mathbb{Z}_+}$ such that $g^t \in \Omega$ and $K(g^t, g^{t+1}) > 0$ for all $t \geq 0$, and there is a $T < \infty$ such that $g^T = \mathbf{o}$. The set of sample paths is denoted by Γ.

The *absorption time* $T : \Gamma \to \mathbb{Z}_+$ of a sample path g is given by

$$T(g) \triangleq \min\{t : g^t = \mathbf{o}\}. \tag{33}$$

Thus for all $g \in \Gamma$, $T(g) < \infty$. Also, $g^t = \mathbf{o}$ and $K(g^t, g^{t+1}) = 1$ for all $t \geq T(g)$. Note that Γ is countable since it is the countable union of the finite sets $\{g : T(g) = t\}$ for $t = 0, 1, 2, \ldots$.

The distribution $\mu_\pi : \mathcal{P}(\Gamma) \to [0, 1]$ on sample paths under the benchmark SIS chain with starting distribution $\pi \in \Delta(\Omega)$ is given, for any $A \in \mathcal{P}(\Gamma)$, by

$$\mu_\pi(A) \triangleq \sum_{g \in A} \pi(g^0) \prod_{t=0}^{T(g)-1} K(g^t, g^{t+1}) \tag{34}$$

and similarly under the distancing chain by

$$\nu_\pi(A) \triangleq \sum_{g \in A} \pi(g^0) \prod_{t=0}^{T(g)-1} K_d(g^t, g^{t+1}). \tag{35}$$

Also, note that Γ is defined to exclude the set of sample paths that are never absorbed, $\{g : g^t \neq \mathbf{o}, \forall t \in \mathbb{Z}_+\}$. These are infinite sequences that never terminate, and therefore

are uncountable. The probabilities μ_π, ν_π, however are well-defined on Γ without such sample paths:

$$\sum_{g\in\Gamma} \mu_\pi(g) = \sum_{t=0}^{\infty} \mu_\pi(\{g : T(g) = t\}) \tag{36}$$

$$= \sum_{s\in\Omega} \pi(s) \sum_{t=0}^{\infty} r_s(Q^t) - r_s(Q^{t+1}) \tag{37}$$

$$= 1 \tag{38}$$

Here, Q is the $2^n - 1 \times 2^n - 1$ sub-stochastic matrix of transition probabilities between non-absorbing states, and $r_s(Q)$ is the s^{th} row-sum of Q. Hence, $r_s(Q^t) - r_s(Q^{t+1})$ is the probability a sample path starting from state s is absorbed at time t. The elements of Q^t approach zero as $t \to \infty$.

Remark 1. $(\Omega, \preceq_\Omega)$ is a partially ordered set. For $s, s' \in \Omega$, $s \preceq_\Omega s'$ if $s_i \leq s'_i$ for all $i \in \mathcal{N}$.

Remark 2. $(\Gamma, \preceq_\Gamma)$ is a partially ordered set. For $h, g \in \Gamma$, $h \preceq_\Gamma g$ if $h^t \preceq_\Omega g^t$ for all $t \in \mathbb{Z}_+$.

Next, we present the main result, which constructs a monotone coupling distribution of ν_π, μ_π by exploiting the differences in node-level transition probabilities.

Theorem 1. Suppose $x, y \in \Omega$ with $x \preceq_\Omega y$. For each $i \in \mathcal{N}$, define $\varphi_i^{x,y} : \{0,1\}^2 \to$

$[0,1]$ according to

$$x_i = y_i = 1, \quad \begin{cases} \varphi_i^{x,y}(0,0) & = \delta(1 - p_{01}^i(y)) \\ \varphi_i^{x,y}(0,1) & = \delta(p_{01}^i(y) - p_{01,d}^i(x)) \\ \varphi_i^{x,y}(1,0) & = 0 \\ \varphi_i^{x,y}(1,1) & = 1 - \delta(1 - p_{01,d}^i(x)) \end{cases} \tag{39}$$

$$x_i = y_i = 0, \quad \begin{cases} \varphi_i^{x,y}(0,0) & = 1 - p_{01}^i(y) \\ \varphi_i^{x,y}(0,1) & = p_{01}^i(y) - p_{01,d}^i(x) \\ \varphi_i^{x,y}(1,0) & = 0 \\ \varphi_i^{x,y}(1,1) & = p_{01,d}^i(x) \end{cases} \tag{40}$$

$$x_i = 0, y_i = 1, \begin{cases} \varphi_i^{x,y}(0,0) & = \delta(1 - p_{01}^i(y)) \\ \varphi_i^{x,y}(0,1) & = 1 - p_{01,d}^i(x) - \delta(1 - p_{01}^i(y)) \\ \varphi_i^{x,y}(1,0) & = 0 \\ \varphi_i^{x,y}(1,1) & = p_{01,d}^i(x) \end{cases} \tag{41}$$

Also, define $\varphi^{x,y} : \Omega^2 \to [0,1]$ for $x \preceq_\Omega y$ by

$$\varphi^{x,y}(\omega, \omega') \triangleq \prod_{i=1}^{n} \varphi_i^{x,y}(\omega_i, \omega_i') \quad \forall \omega, \omega' \in \Omega. \tag{42}$$

Lastly, define $\Phi_\pi : \Gamma^2 \to [0,1]$ for any $\pi \in \Delta(\Omega)$ by

$$\Phi_\pi(h, g) \triangleq \chi(h^0 = g^0)\pi(h^0) \prod_{t=0}^{T(g)-1} \varphi^{h^t, g^t}(h^{t+1}, g^{t+1}). \tag{43}$$

Then Φ_π is a monotone coupling of ν_π, μ_π.

Proof. See Appendix. ■

The coupling between node-level transition probabilities $\varphi_i^{x,y}$ given in (39)-(41) are used to establish a coupling between benchmark and distancing probability distributions on sample paths. The form of the $\varphi_i^{x,y}$ is identical to the method in which

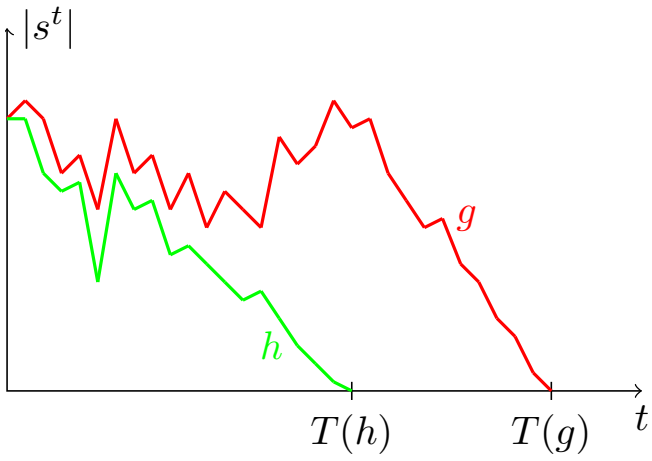

Figure 8: A pair of sample paths (h, g) drawn from Φ_π.

two biased coins are coupled in (26). When the coupling rule is applied to each node's probability of infection, it ensures no node can be infected in the distancing chain while being susceptible in the benchmark chain. Consequently, the monotone coupling Φ_π is a distribution on pairs of sample paths (h, g) satisfying $h^0 = g^0$, $h \preceq_\Gamma g$ (see Figure 8) and marginally, $h \sim \nu_\pi$, $g \sim \mu_\pi$. The next result characterizes the difference between μ_π and ν_π-expectations of any non-negative increasing function on the sample paths Γ with respect to the coupling distribution Φ_π.

Corollary 1. For any increasing $\mathbb{Z}_+$-valued random variable Z in Γ,

$$\mathbb{E}_{\mu_\pi}(Z) - \mathbb{E}_{\nu_\pi}(Z) = \sum_{\tau=0}^{\infty} \Phi_\pi(Z_\tau^c, Z_\tau). \tag{44}$$

where $Z_\tau = \{x \in \Gamma : Z(x) > \tau\}$.

Proof. Immediate from Theorem 1 and Proposition 1. ■

One can think of an increasing $Z : \Gamma \to \mathbb{Z}_+$ as an epidemic cost metric. Here, $\Phi_\pi(Z_\tau^c, Z_\tau)$ is simply the probability a benchmark sample path g incurs a cost greater than τ, while the corresponding distancing sample path h costs less than τ, where $(h, g) \sim \Phi_\pi$. Some examples of increasing $\mathbb{Z}_+$-valued random variables in Γ are

- The absorption time $T : \Gamma \to \mathbb{Z}_+$, defined by (33).

- Cumulative infected individuals up to time m, defined by $g \mapsto \sum_{t=0}^{m} |g^t|$, where $|s| \triangleq \sum_{i \in \mathcal{N}} s_i$ for $s \in \Omega$.

- The "epidemic spread", or how many unique nodes that contract the disease in a given amount of time m. This is given by $g \mapsto \sum_{i \in \mathcal{N}} \chi_{E_i}(g)$, where $E_i = \{g : \sum_{t=0}^{m} g_i^t > 0\}$.

The difference (44) encodes many complex dependencies on the epidemic parameters δ and β, the awareness weight α, and the structure of the graphs $\mathcal{G}_C$ and $\mathcal{G}_I$.

The following result establishes stochastic domination of the distancing chain by the benchmark chain.

Corollary 2. The benchmark chain stochastically dominates the distancing chain on sample paths, i.e. $\mu_\pi \succeq \nu_\pi$.

Proof. For any upper set $\mathcal{I} \subset \Gamma$, $\chi_{\mathcal{I}}(\cdot)$ is increasing in Γ. By (44),

$$\begin{aligned} \mu_\pi(\mathcal{I}) - \nu_\pi(\mathcal{I}) &= \mathbb{E}_{\mu_\pi}(\chi_{\mathcal{I}}) - \mathbb{E}_{\nu_\pi}(\chi_{\mathcal{I}}) \\ &= \Phi_\pi(\mathcal{I}^c, \mathcal{I}) \geq 0 \end{aligned} \tag{45}$$

■

This result affirms the intuition that sample paths with consistently higher numbers of infected individuals occur with higher probability in the benchmark chain than in the distancing chain.

4.3 Summary

In this chapter, we proved that the expectation of any epidemic cost metric is lower under the distancing Markov chain, an intuitive result. However, to do so, we invoked a monotone coupling argument, where an auxiliary stochastic process on pairs of sample paths was defined. The reduction in expectations is given in closed form in terms of the monotone coupling distribution. Drawing from the conclusions of

Chapter 2, one would expect an endemic state to exist in the networked model under certain conditions. However, an absorbing Markov chain analysis does not offer any notion of a "metastable" equilibrium. In the next chapter, this intuition is formalized under a mean-field approximation of the Markov chain models.

CHAPTER V

EXISTENCE OF AN ENDEMIC STATE

The analysis of Chapter 4 gives little interpretation of the medium-term behavior of either benchmark or awareness models. As stated before, Markov chain theory says the chain is absorbed in finite time with probability one, so it does not reveal the metastability properties (i.e. the endemic state) that arise in the transient period before absorption. This chapter resolves this shortcoming by presenting stability properties of a mean-field approximation (MFA) of the Markov chain dynamics. The main result of this Chapter is analogous to the stability properties of the ODE awareness model studied in Chapter 1.

5.1 Derivation of mean-field approximations

In this section, a mean-field approximation is derived for both benchmark and awareness models. The MFA's are deterministic, discrete-time dynamic systems with an n-dimensional state space $[0,1]^n$, which is interpreted to be each node's probability of being infected at any given time.

Here, $s^t \in \Omega$ is the epidemic state at time $t = 0, 1, \ldots$. Indeed, consider the awareness chain whose node-level stochastic state transition update obeys

$$s_i^{t+1} = s_i^t B(1 - \delta p_{00,d}^i(s^t)) + (1 - s_i^t) B(p_{01,d}^i(s^t)) \tag{46}$$

where $B(\lambda)$ denotes a Bernoulli random variable with parameter $\lambda \in [0,1]$. For shorthand, denote $x_i^t \triangleq \Pr(s_i^t = 1)$ for the probability node i is infected at time t.

Taking the probability of both sides equaling one,

$$\begin{aligned} x_i^{t+1} &= \Pr(B(1-\delta p_{00,d}^i(s^t))=1|s_i^t=1)\Pr(s_i^t=1) + \Pr(B(p_{01,d}^i(s^t))=1|s_i^t=0)\Pr(s_i^t=0) \\ &= x_i^t(1-\delta p_{00,d}^i(s^t)) + (1-x_i^t)p_{01,d}^i(s^t) \\ &= x_i^t(1-\delta) + (1-(1-\delta)x_i^t)p_{01,d}^i(s^t) \end{aligned} \tag{47}$$

Note the expression for x_i^{t+1} still depends stochastically on the state s^t. To obtain a mean-field approximation of x_i^{t+1}, simply replace the state s^t with x^t (the n-vector with components x_i^t) in (47). Thus, by redefining x_i^{t+1} to obey this approximation and extending the domain of $\mu_i(\cdot), a_i(\cdot)$ and $p_{01,d}^i(\cdot)$ from $\{0,1\}^n$ to $[0,1]^n$, the following approximate dynamics

$$x_i^{t+1} = x_i^t(1-\delta) + (1-(1-\delta)x_i^t)p_{01,d}^i(x^t) \tag{48}$$

describe the time evolution of node i's probability of being infected. Stacking the dynamics for every node into a vector, we obtain a mapping $\phi : [0,1]^n \to [0,1]^n$ where $\phi_i(x) = x_i(1-\delta) + (1-(1-\delta)x_i)p_{01,d}^i(x)$ and $x^{t+1} = \phi(x^t)$. This MFA of the distancing chain is in contrast to the MFA of the benchmark chain,

$$x_i^{t+1} = x_i^t(1-\delta) + (1-(1-\delta)x_i^t)p_{01}^i(x^t) \tag{49}$$

which is studied thoroughly in [1]. It is derived in the same manner, and is described by the mapping $\psi : [0,1]^n \to [0,1]^n$ with $\psi_i(x) = x_i(1-\delta) + (1-(1-\delta)x_i)p_{01}^i(x)$ and $x^{t+1} = \psi(x^t)$.

The two mappings ϕ and ψ are nonlinear, continuous mappings satisfying $\phi(x) \prec \psi(x)$ for $x \in [0,1]^n \backslash \mathbf{0}_n$, $\phi(\mathbf{0}_n) = \psi(\mathbf{0}_n) = \mathbf{0}_n$. Linearization of ϕ and ψ about the origin yields the same Jacobian matrix, $\beta A_C + (1-\delta)I$, and hence the same linearized dynamics $x^{t+1} = (\beta A_C + (1-\delta)I)x^t$. The linear dynamics serve as an upper bound to both (48) and (49). Therefore, if $\lambda_{\max}(\beta A_C + (1-\delta)I) < 1$, the origin is a globally stable fixed point and it is an unstable fixed point if $\lambda_{\max}(\beta A_C + (1-\delta)I) > 1$.

Figure 9 suggests the MFA dynamics concur with the Markov chains, with the awareness MFA slightly overestimating its stochastic analogue.

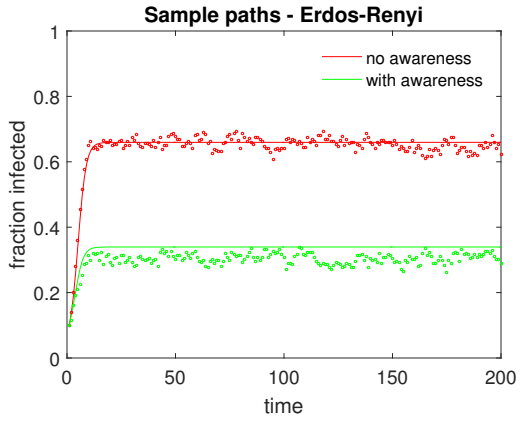

Figure 9: A pair of sample paths generated from the Markov chain models (points) and the MFA (solid lines) dynamics (48),(49). Here, $\beta = 0.1, \delta = 0.5, \alpha = 1$, and $\mathcal{G}_I = \mathcal{G}_C$. Performed on a 1000 node Erdős-Renyi network with parameter $p = 0.01$.

5.2 Epidemic threshold condition

We now provide a sufficient condition for the existence of a non-trivial fixed point ($\succ \mathbf{0}_n$, the n-vector of zeros) of ϕ.

Theorem 2. If $\lambda_{\max}(\beta A_C + (1-\delta)I_n) > 1$, there exists a nontrivial fixed point for ϕ.

The existence of such a fixed point suggests the epidemic has a metastable endemic state, where the spread of the disease is fast enough to sustain an epidemic in the network. Our condition coincides with the condition for existence, uniqueness, and global asymptotic stability of the non-trivial fixed point q^* of ψ, which is $\lambda_{\max}(\beta A_C + (1-\delta)I) > 1$, i.e. when the origin in the linearized dynamics is unstable (Theorem 5.1, [1]). This condition incorporates the factors that contribute to the rate of spreading - δ, β, and the contact network A_C. The proof makes use of the following lemmas.

Lemma 1 (Lemma 3.1, [1]). There exists a vector $\nu \succ 0_n$ such that $(\beta A_C - \delta I_n)\nu \succ 0_n$ if and only if $\lambda_{\max}(\beta A_C + (1-\delta)I_n) > 1$.

The connectedness assumption for $\mathcal{G}_C$ is necessary for the above Lemma because the proof applies the Perron-Frobenius theorem for nonnegative irreducible matrices. The next result is an equivalent formulation of Brouwer's fixed point theorem.

Lemma 2. (Theorem 4.2.3, [14]): Suppose $f_i : D_n \to \mathbb{R}, i = 1, \ldots, n$ are continuous mappings, where

$$D_n = \{x \in \mathbb{R}^n : x_i \in [\ell_i, u_i], \forall i\}$$

for real numbers ℓ_i, u_i. We also define the set

$$D_{-i} = \{x_{-i} \in \mathbb{R}^{n-1} : x_j \in [\ell_j, u_j] \ \forall j \neq i\}$$

If for every i and for all $x_{-i} \in D_{-i}$,

$$f_i(x_1, \ldots, \ell_i, \ldots, x_n) = f_i(x_{-i}, \ell_i) \geq 0 \tag{50}$$

$$f_i(x_1, \ldots, u_i, \ldots, x_n) = f_i(x_{-i}, u_i) \leq 0, \tag{51}$$

then there exists a point $x^* \in D_n$ such that $f_i(x^*) = 0$, for all $i = 1, \ldots, n$.

The final lemma needed is a technical result for the mean-field mappings ϕ_i.

Lemma 3. For each $i \in \mathcal{N}$, define the maps $f_i : [0,1]^n \to \mathbb{R}$ by

$$\begin{aligned} f_i(x) &\triangleq \phi_i(x) - x_i \\ &= -\delta x_i + (1 - (1-\delta)x_i) p^i_{01,d}(x) \end{aligned} \tag{52}$$

Then for any $i \in \mathcal{N}$ and $x_{-i} \in [0,1]^{n-1}$, the function $f_i(x_{-i}, \cdot)$ has a unique root $c_i^*(x_{-i}) \in [0,1)$ which depends continuously on x_{-i}. Furthermore, one can find a sequence $x^k_{-i} \to \mathbf{0}_{n-1}$ s.t. $c_i^*(x^k_{-i})$ is monotonically decreasing to 0.

Proof. For any $i \in \mathcal{N}$ and $x_{-i} \in [0,1]^{n-1}$,

$$f_i(x_{-i}, 0) = p^i_{01,d}(x_{-i}, 0) \geq 0. \tag{53}$$

and

$$f_i(x_{-i}, 1) = \delta(p^i_{01,d}(x_{-i}, 1) - 1) < 0. \tag{54}$$

The function $f_i(x_{-i}, \cdot)$ is strictly decreasing: for $a, b \in [0,1]$ s.t. $a < b$, $f_i(x_{-i}, a) - f_i(x_{-i}, b)$ is given by

$$\begin{aligned}(b-a)(\delta + (1-\delta)p^i_{01,d}(x_{-i}, b)) + \cdots \\ + (1 - a(1-\delta))(p^i_{01,d}(x_{-i}, a) - p^i_{01,d}(x_{-i}, b)) \\ > 0.\end{aligned}$$

This follows because $p^i_{01,d}(x_{-i}, x_i)$ is decreasing in x_i (x_i contributes to global awareness). Hence for every $x_{-i} \in [0,1]^{n-1}$, there is a unique $c^*_i(x_{-i}) \in [0,1)$ s.t. $f_i(x_{-i}, c^*_i(x_{-i})) = 0$, and $c^*_i(x_{-i})$ depends continuously on x_{-i}. To see this, observe that $c^*_i(x_{-i}) \in [0,1)$ is a root of the equation

$$(1 - (1-\delta)x_i)\left(1 - \prod_{j \in \mathcal{N}^C_i} (1 - a_i(x_{-i}, x_i)\beta x_j)\right) - \delta x_i = 0, \tag{55}$$

which is a polynomial in x_i. The coefficients of the polynomial depend continuously on $x_{-i} \in [0,1]^{n-1}$, and the roots of any polynomial are continuous with respect to its coefficients. Consequently, for any sequence $x^k_{-i} \to \mathbf{0}_{n-1}$, $c^*_i(x^k_{-i}) \to c^*_i(\mathbf{0}_{n-1}) = 0$ by continuity. This allows us to select a subsequence of x^k_{-i} such that c^*_i is monotonically decreasing along the subsequence. ■

We are now ready to prove the main result of this section.

Proof of Theorem 2: Let the mappings f_i, $i \in \mathcal{N}$ be as in Lemma 3. We need to verify (50) and (51) hold for all i and for choices of ℓ_i, u_i satisfying $0 < \ell_i < u_i$. This ensures the awareness dynamic ϕ has a fixed point other than the origin. Choose $u_i = u$ where u satisfies

$$\max_{i \in \mathcal{N}} \max_{x_{-i} \in [0,1]^{n-1}} c^*_i(x_{-i}) < u < 1. \tag{56}$$

Then for all $x_{-i} \in [0,u]^{n-1}$,

$$f_i(x_{-i}, u) < 0 \tag{57}$$

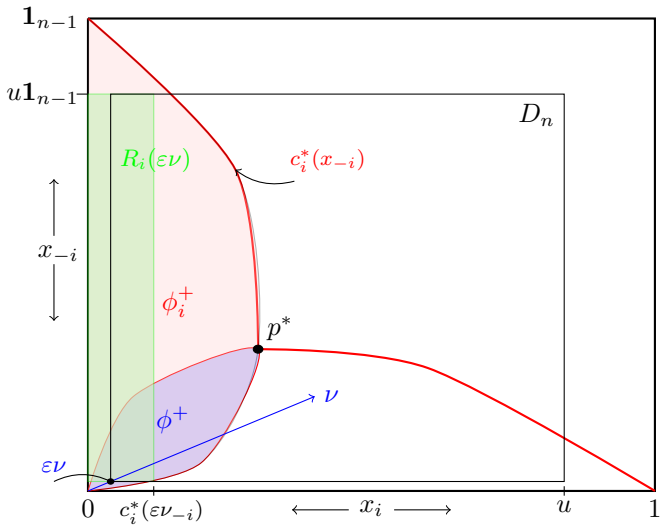

Figure 10: Diagram of the proof. Here, p^* denotes a nontrivial fixed point of ϕ.

since $u > c_i^*(x_{-i})$. Thus, (51) holds, regardless of the choice of ℓ_i. However, it remains to find the $\ell_i > 0$ s.t. (50) is satisfied. Let $f(x) \triangleq [f_1(x), \ldots, f_n(x)]^T$ and define the sets

$$\phi_i^+ \triangleq \{x \in [0,1]^n : f_i(x) \geq 0\}, \quad \phi^+ \triangleq \bigcap_{j=1}^{n} \phi_j^+ \tag{58}$$

The Jacobian of f about the origin is $(\beta A_C - \delta I_n)$. By Lemma 1, there exists a vector $\nu \succ \mathbf{0}_n$ such that $(\beta A_C - \delta I_n)\nu \succ \mathbf{0}_n$. Consequently for sufficiently small $\varepsilon > 0$,

$$f(\varepsilon\nu) \succ \mathbf{0}_n, \tag{59}$$

or $\varepsilon\nu \in \phi^+$. We also define the set

$$R_i(x) \triangleq \{y \in \mathbb{R}^n : y_i \in [0, c_i^*(x_{-i})], y_j \in [x_j, u], j \neq i\} \tag{60}$$

If $\varepsilon\nu_i \leq c_i^*(\varepsilon\nu_{-i})$ and $R_i(\varepsilon\nu) \subset \phi_i^+$, then (50) is satisfied, i.e. $f_i(x_{-i}, \varepsilon\nu_i) \geq 0$ on $D_{-i} = \{\varepsilon\nu_{-i} \preceq x_{-i} \preceq u\mathbf{1}_{n-1}\}$ for ε sufficiently small. We already have $\varepsilon\nu_i \leq c_i^*(\varepsilon\nu_{-i})$ because $\varepsilon\nu \in \phi^+ \subset \phi_i^+$. To show $R_i(\varepsilon\nu) \subset \phi_i^+$, by Lemma 3 we can find a sequence $\varepsilon_k\nu \in \phi^+$ with $\varepsilon_k \to 0$ s.t. $c_i^*(\varepsilon_k\nu_{-i})$ is monotonically decreasing to 0. By stopping at a large enough k, we can essentially take a ε small enough such that

$$c_i^*(\varepsilon\nu_{-i}) = \min_{x_{-i} \in D_{-i}} c_i^*(x_{-i}) \tag{61}$$

Consequently, $R_i(\varepsilon\nu) \subset \phi_i^+$. Choosing ε small enough to satisfy this for all $i \in \mathcal{N}$ verifies (50) by using $D_n = \{x \in \mathbb{R}^n : x_j \in [\varepsilon\nu_j, u]\}$. See Figure 10 for an illustration of the proof. By Lemma 2, ϕ has a fixed point contained in D_n. ■

The condition of Theorem 2 is independent of the awareness parameter α and the structure of the information network $\mathcal{G}_I$. Hence, social distancing alone cannot restore stability of the disease-free equilibrium point. However, social distancing lowers the overall metastable state of an epidemic.

Corollary 3. If $q^* \succ \mathbf{0}_n$ is the unique nontrivial fixed point of ψ, then any nontrivial fixed point p^* of ϕ satisfies $p^* \prec q^*$.

Proof. Define the sets ψ_i^+ and ψ^+ similarly as in (58). It was shown in [1] that q^* is the unique maximal element of ψ^+, i.e $q^* \succ q$, $\forall q \in \psi^+$, $q \neq q^*$. Observe $\phi(x) \prec \psi(x)$ for any $x \in [0,1]^n \backslash \mathbf{0}_n$. Let $x \in \phi^+$, $x \neq \mathbf{0}_n$. Then $x \preceq \phi(x) \prec \psi(x)$, so $x \in \psi^+$. Therefore, $\phi^+ \subset \psi^+$. ■

5.3 Summary

The existence result of this Chapter mirrors the result of adding awareness to the SIS ODE model in Chapter 1. The addition of awareness and social distancing lowers the final epidemic size, but does not improve upon the threshold for epidemic persistence. Social distancing is a decentralized mechanism that mitigates the severity of an epidemic. In the networked case, we have not proven uniqueness or stability of the nontrivial fixed point. We also do not have a closed-form expression for the final epidemic size due to the high dimensionality and nonlinearity of the model (recall in Chapter 1 that $\hat{I} = N(1 - \sqrt{\delta/\beta})$). Despite these analytical shortcomings, the numerical simulations of the next Chapter suggest that the nontrivial fixed point of the awareness MFA is unique and globally stable for all the cases studied. A characterization of the fixed points for different random graph families is given in Chapter 6.

CHAPTER VI

SIMULATIONS ON RANDOM GRAPHS

In this chapter, we illustrate through numerical simulations how the structure of the contact network $\mathcal{G}_C$ affects the course of an epidemic in the presence of awareness and social distancing. Extensive analytical and simulation studies have been conducted without awareness ([39],[12],[8],[37],[27]).

6.1 Random contact and social networks

Here, we consider contact networks from three random graph families - geometric, Erdős-Renyi, and scale-free. These networks are relevant in studying epidemic spreading because they exhibit a variety of qualitative features that reflect real-world networks. Geometric networks portray people connected by geographic distance. Erdős-Renyi random networks display a small-world effect common in many real world networks - e.g neural and social influence networks. Online social networks and the World Wide Web are examples of scale-free networks [22].

A geometric random network is generated by placing n points uniformly at random on the unit torus (unit square with periodic boundary conditions). An edge exists between any two points if they are less than a specified Euclidean distance $r \in (0, 1)$ away. Erdős-Renyi random graphs are constructed by forming an edge between any two nodes independently with a fixed probability $p_{\text{ER}} \in (0, 1)$. Scale-free networks are generated by the preferential attachment algorithm [3] as follows. Starting with an initial connected graph of $m_0 \geq m$ nodes, $n - m_0$ additional nodes are added sequentially, with each incoming node establishing links to m existing nodes in the network. The probability an existing node receives an incoming link is proportional to its degree. We performed simulation analysis on one network from each random

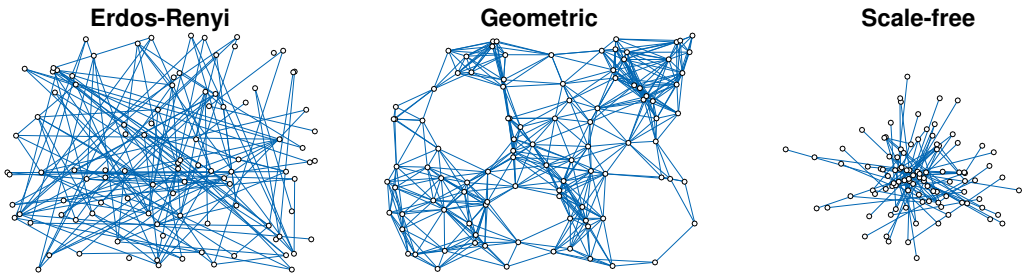

(a) Erdős-Renyi (b) Geometric (c) Scale-free

Figure 11: Example contact networks from three random graph families.

graph family. The networks all have 1000 nodes with an average degree of 10, and hence the same number of edges. In our model, the social network $\mathcal{G}_I$ is generated directly from $\mathcal{G}_C$ via a parameter $p \in (0, 1)$ through the following procedure: 1) Select a fraction p of existing edges in $\mathcal{E}_C$ at random and remove them from the edge set; 2) For each of the selected edges, select one of the two end nodes randomly (e.g with probability 1/2) as the root node; 3) For each of the selected root nodes i, select $j \neq i$ uniformly at random and add the edge (i, j). For p close to one, the resulting graph $\mathcal{G}_I = (\mathcal{N}, \mathcal{E}_I)$ exhibits the small-world effect (small average shortest path length and small clustering) [41]. When $p = 0$, $\mathcal{G}_I = \mathcal{G}_C$.

6.2 Epidemic dynamics on random networks

In Figure 12, the normalized non-trivial fixed points are characterized for the three random networks in the interval of epidemic persistence ($\delta/\beta \in [0, \lambda_{\max}(A_C)]$). The fixed points (solid lines) are computed by iterating the MFA dynamics (48) and (49) with an arbitrary initial condition until convergence. The stochastic long-run infected fractions (diamonds) are computed by averaging the levels of epidemic states in the latter half of a sample run of length 200. The norms of the MFA fixed points approximate the size of the endemic states and they slightly overestimate the actual long-run infected fraction observed in stochastic simulations of the Markov chains. The vertical dashed lines indicate $\lambda_{\max}(A_C)$. The Erdős-Renyi network of Figure 12a

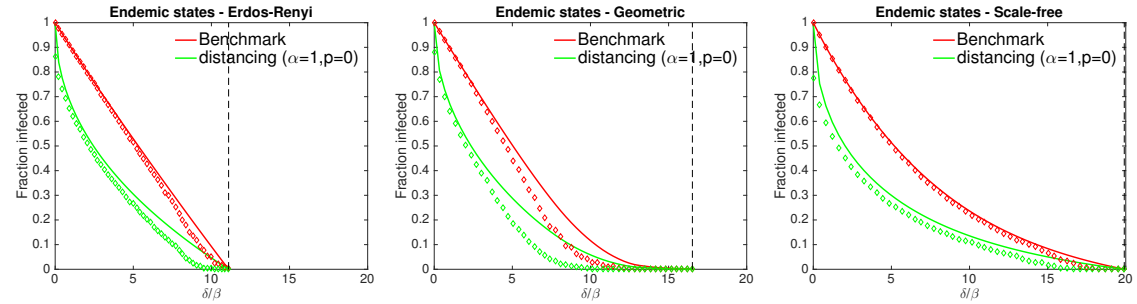

(a) (b) (c)

Figure 12: Characterization of fixed points for three random graphs.

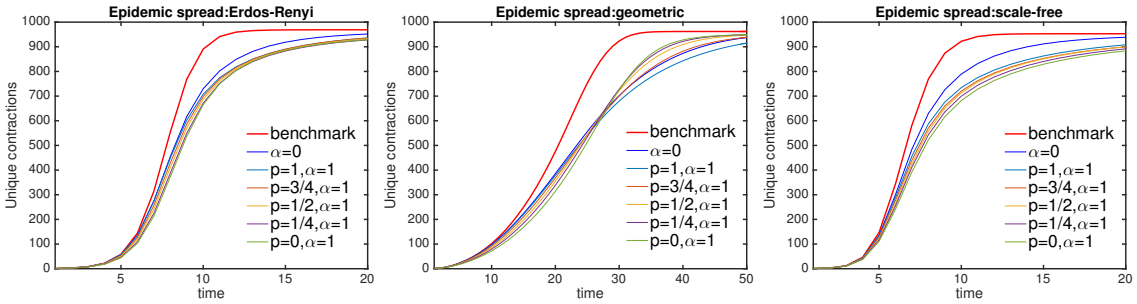

(a) (b) (c)

Figure 13: Epidemic spreading as a function of time (same networks as Fig. 12).

is connected and has parameter $p_{\text{ER}} = .01$ with $\lambda_{\max}(A_C) = 11.1$. The geometric random network in Figure 12b has connectivity radius $r = .0564$ with $\lambda_{\max}(A_C) = 16.52$. Lastly, the network in Figure 12c is generated from the preferential attachment algorithm with $m = 5$, and $\lambda_{\max}(A_C) = 19.9$.

In Figure 13, we quantify the "epidemic spread" by the number of unique nodes that contract an infection as time progresses when one node chosen uniformly at random is initially infected. This metric is an example of an increasing random variable over sample paths (Chapter 4) and is helpful in revealing not only how fast an epidemic initially spreads in the network, but also how far-reaching it is. A key observation is that contact awareness ($p = 0, \alpha = 1$) slows epidemic spreading better than any other awareness configuration at the beginning of an epidemic. This is intuitively clear since contact awareness provides nodes with the most vital information if they are in danger of getting infected, whereas global information alone would not

inform agents of impending danger. As p increases, $\mathcal{G}_I$ deviates more from $\mathcal{G}_C$ and the information nodes receive become less vital.

Erdős-Renyi and scale-free (with $m = 5$) networks admit disease spread throughout the entire network in a short amount of time, even with social distancing (Figure 13a,13c). This is attributed to small average shortest path lengths (Ch. 8 & 12, [22]), allowing the epidemic to quickly spread to other parts of the network. Random geometric networks are characterized by high clustering and large diameter. Clustering slows the spread of an epidemic (Figure 13b), but also contributes to increasing the final epidemic size [38]. The disease stays localized and spreads slowly. This explains the inversion of awareness parameters in Figure 13b. By the time the epidemic first reaches its endemic level around $t = 20$, many nodes have not yet been exposed because at this point their local communities are untouched. Thus, having global or long-range social awareness (low α or high p) is more beneficial over contact awareness.

6.3 Summary

In this chapter, we investigated to what extent awareness and social distancing mitigates an epidemic on various random graphs. The structure of the graph plays an important role, as shown in the fixed point profiles of three different random graphs (Figure 12), and the progression of the epidemic spread (Figure 13). Consistent with the conclusions of chapter 5, the endemic state in the simulations vanishes once $\delta/\beta > \lambda_{\max}(A_C)$.

CHAPTER VII

CONCLUSION

This thesis studies the effect individual awareness and social distancing has on mitigating an epidemic. A simple SIS ordinary differential equation model is initially presented and analyzed in Chapter 2. It is slightly modified to incorporate an element of social distancing. The stability properties of both models coincide. That is, the all-susceptible state is stable when $\delta > \beta$ and the endemic state is stable otherwise. However, the endemic state in the awareness model is strictly lower than that in the original model.

In Chapter 3, the networked SIS epidemic models with and without awareness are introduced as finite-state, discrete-time Markov chains. On top of the physical contact network in which the disease spreads, the nodes are connected socially on a separate network. An individual, or node on the network, receives information about the epidemic from its social contacts and a global broadcast of the total number of infected nodes. Based on the level of threat an individual perceives, it reacts by proportionally reducing contact with its neighbors.

A full stochastic comparison analysis between benchmark and awareness network models is presented in Chapter 4. Through a monotone coupling framework, we show the benchmark chain stochastically dominates the awareness chain on the space of sample paths. As a result, we are able to prove the awareness chain reduces the expectation of any epidemic metric (increasing random variable over sample paths) - e.g. the eradication time, total infected over time, and the epidemic spread metric.

In Chapter 5, the conclusions drawn from the ODE models are shown to analytically generalize to SIS epidemics on networks. This is done by deriving a mean-field

approximation of the Markov chain dynamics to obtain a set of n coupled difference equations. It is then shown that the condition for existence of a nontrivial fixed point in the awareness model coincides with the condition for the benchmark model.

Simulations on three different random graphs are given in Chapter 6. The qualitative aspects of the network structure affects how quickly an epidemic spreads throughout a network and the overall composition of the endemic state. With awareness, some network topologies are able to restrict spreading better than others.

APPENDIX A

PROOFS

Proof of Theorem 1. When $x \preceq_\Omega y$, the $\varphi_i^{x,y}$ are well-defined probabilities since $p_{01}^i(y) - p_{01,d}^i(x) \geq 0$ and $1 - p_{01,d}^i(x) - \delta(1 - p_{01}^i(y)) > 0$. One can see by inspection that $\varphi_i^{x,y}$ is a monotone coupling of $\mathbb{P}_i^d(x,\cdot)$ and $\mathbb{P}_i(y,\cdot)$ defined in (22), (23) and (16), (17) respectively.

Observe from (42), $\varphi^{x,y}(\omega,\omega') > 0$ implies $x \preceq_\Omega y$ and $\omega \preceq_\Omega \omega'$. Consequently, $\varphi^{x,y}$ is a monotone coupling of $K_d(x,\cdot), K(y,\cdot)$:

$$\begin{aligned}\sum_{\omega' \succeq_\Omega \omega} \varphi^{x,y}(\omega,\omega') &= \sum_{\omega_1' \geq \omega_1} \varphi_1^{x,y}(\omega_1,\omega_1') \sum_{\omega_2' \geq \omega_2} \varphi_2^{x,y}(\omega_2,\omega_2') \cdots \sum_{\omega_n' \geq \omega_n} \varphi_n^{x,y}(\omega_n,\omega_n') \\ &= \prod_{i=1}^n \mathbb{P}_i^d(x,\omega_i) \qquad (62) \\ &= K_d(x,\omega) \qquad (63)\end{aligned}$$

By a completely analogous computation, we obtain $\sum_{\omega' \preceq_\Omega \omega} \varphi^{x,y}(\omega',\omega) = K(y,\omega)$.

Also, notice from (43) that $\Phi_\pi(h,g) > 0$ implies $h^0 = g^0$ and $h \preceq_\Gamma g$. Consequently, Φ_π is a monotone coupling of ν_π, μ_π:

$$\begin{aligned}\sum_{g \succeq_\Gamma h} \Phi_\pi(h,g) &= \sum_{\substack{g \succeq_\Gamma h \\ g^0 = h^0}} \pi(h^0) \prod_{t=0}^{T(g)-1} \varphi^{h^t,g^t}(h^{t+1},g^{t+1}) \qquad (64) \\ &= \pi(h^0) \sum_{g^1 \succeq h^1} \varphi^{h^0,g^0}(h^1,g^1) \ \cdots \sum_{g^{T(h)} \succeq \{0\}^n} \varphi^{h^{T(h)-1},g^{T(h)-1}}(\mathbf{o},g^{T(h)}) \qquad (65) \\ &= \pi(h^0) \prod_{t=1}^{T(h)} \sum_{g^t \succeq_\Omega h^t} \varphi^{h^{t-1},g^{t-1}}(h^t,g^t) \qquad (66) \\ &= \pi(h^0) K_d(h^0,h^1) K_d(h^1,h^2) \cdots K_d(h^{T(h)-1},\mathbf{o}) \qquad (67) \\ &= \nu_\pi(h) \qquad (68)\end{aligned}$$

The equality (65) is the combinatorial form of writing (64), and the product terminates at $T(h)$ because 1) $g \succeq_\Gamma h$ implies $T(g) \geq T(h)$, 2) $h^t = \mathbf{o}$ for all $t \geq T(h)$ and 3) for any $t > T(h)$,

$$\sum_{g^t \succeq_\Omega h^t} \varphi^{h^{t-1}, g^{t-1}}(h^t, g^t) = \sum_{g^t \in \Omega} \varphi^{\mathbf{o}, g^{t-1}}(\mathbf{o}, g^t) = K_d(\mathbf{o}, \mathbf{o}) = 1$$

By an analogous computation, $\sum_{h \preceq_\Gamma g} \Phi_\pi(h, g) = \mu_\pi(g)$:

$$\begin{aligned}
\sum_{h \preceq_\Gamma g} \Phi_\pi(h, g) &= \sum_{\substack{h \preceq_\Gamma g \\ g^0 = h^0}} \pi(g^0) \prod_{t=0}^{T(g)-1} \varphi^{h^t, g^t}(h^{t+1}, g^{t+1}) \\
&= \pi(g^0) \sum_{h^1 \preceq g^1} \varphi^{h^0, g^0}(h^1, g^1) \ \cdots \sum_{h^{T(g)} \preceq \{0\}^n} \varphi^{h^{T(g)-1}, g^{T(g)-1}}(h^{T(g)}, \mathbf{o}) \\
&= \pi(g^0) K(g^0, g^1) K(g^1, g^2) \cdots K(g^{T(g)-1}, \mathbf{o}) \\
&= \mu_\pi(g) \qquad (69)
\end{aligned}$$

■

REFERENCES

[1] Ahn, H. J. and Hassibi, B., "Global dynamics of epidemic spread over complex networks," in *Decision and Control (CDC), 2013 IEEE 52nd Annual Conference on*, pp. 4579–4585, Dec 2013.

[2] Ahn, H. J. and Hassibi, B., "On the mixing time of the sis markov chain model for epidemic spread," in *Decision and Control (CDC), 2014 IEEE 53rd Annual Conference on*, pp. 6221–6227, Dec 2014.

[3] Barabási, A.-L. and Albert, R., "Emergence of scaling in random networks," *Science*, vol. 286, no. 5439, pp. 509–512, 1999.

[4] Bauch, C. T. and Earn, D. J. D., "Vaccination and the theory of games," *Proceedings of the National Academy of Sciences of the United States of America*, vol. 101, no. 36, pp. 13391–13394, 2004.

[5] Bauch, C. T. and Galvani, A. P., "Social factors in epidemiology," *Science*, vol. 342, no. 6154, pp. 47–49, 2013.

[6] Bodine-Baron, E., Bose, S., Hassibi, B., and Wierman, A., "Minimizing the social cost of an epidemic," in *Game Theory for Networks* (Jain, R. and Kannan, R., eds.), vol. 75 of *Lecture Notes of the Institute for Computer Sciences, Social Informatics and Telecommunications Engineering*, pp. 594–607, Springer Berlin Heidelberg, 2012.

[7] Drakopoulos, K., Ozdaglar, A., and Tsitsiklis, J., "An efficient curing policy for epidemics on graphs," in *Decision and Control (CDC), 2014 IEEE 53rd Annual Conference on*, pp. 4447–4454, Dec 2014.

[8] Eguíluz, V. M. and Klemm, K., "Epidemic threshold in structured scale-free networks," *Phys. Rev. Lett.*, vol. 89, p. 108701, Aug 2002.

[9] Funk, S., Gilad, E., and Jansen, V., "Endemic disease, awareness, and local behavioural response," *Journal of Theoretical Biology*, vol. 264, no. 2, pp. 501 – 509, 2010.

[10] Funk, S., Gilad, E., Watkins, C., and Jansen, V. A. A., "The spread of awareness and its impact on epidemic outbreaks," *Proceedings of The National Academy of Sciences*, vol. 106, pp. 6872–6877, 2009.

[11] Funk, S., Salathé, M., and Jansen, V. A. A., "Modelling the influence of human behaviour on the spread of infectious diseases: a review," *Journal of The Royal Society Interface*, 2010.

[12] Ganesh, A., Massoulie, L., and Towsley, D., "The effect of network topology on the spread of epidemics," in *INFOCOM 2005. 24th Annual Joint Conference of the IEEE Computer and Communications Societies. Proceedings IEEE*, vol. 2, pp. 1455–1466 vol. 2, March 2005.

[13] Grinstead, C. and Snell, J., *Introduction to Probability*. American Mathematical Society, 1997.

[14] Istratescu, V. I., *Fixed Point Theory, An Introduction*. Holland: D.Reidel, 1981.

[15] Keeling, M. and Rohani, P., *Modeling Infectious Diseases in Humans and Animals*. Princeton, NJ: Princeton University Press, 2011.

[16] Kermack, W. O. and McKendrick, A. G., "A contribution to the mathematical theory of epidemics," *Proceedings of the Royal Society of London A: Mathematical, Physical and Engineering Sciences*, vol. 115, no. 772, pp. 700–721, 1927.

[17] Khalil, H. K., *Nonlinear Systems*. New Jersey: Prentice Hall, 2002.

[18] Levin, D., Peres, Y., and Wilmer, E., *Markov Chains and Mixing Times*. American Mathematical Soc.

[19] Lindvall, T., *Lectures on the Coupling Method*. Dover Books on Mathematics Series, Dover Publications, Incorporated, 2002.

[20] Molina, C. and Earn, D. J. D., "Game theory of pre-emptive vaccination before bioterrorism or accidental release of smallpox," *Journal of The Royal Society Interface*, vol. 12, no. 107, 2015.

[21] Ndeffo Mbah, M. L., Liu, J., Bauch, C. T., Tekel, Y. I., Medlock, J., Meyers, L. A., and Galvani, A. P., "The impact of imitation on vaccination behavior in social contact networks," *PLoS Comput Biol*, vol. 8, p. e1002469, 04 2012.

[22] Newman, M., *Networks: An Introduction*. New York, NY, USA: Oxford University Press, Inc., 2010.

[23] Omic, J., Orda, A., and Van Mieghem, P., "Protecting against network infections: A game theoretic perspective," in *INFOCOM 2009, IEEE*, pp. 1485–1493, April 2009.

[24] Omic, J., *Epidemics in networks: modeling, optimization and security games*. PhD thesis, Delft University of Technology, 2010.

[25] Paarporn, K., Eksin, C., Weitz, J., and Shamma, J. S., "Epidemic spread over networks with agent awareness and social distancing," in *53rd Annual Allerton Conference on Communication, Control, and Computing*, 2015.

[26] Pandey, A., Atkins, K. E., Medlock, J., Wenzel, N., Townsend, J. P., Childs, J. E., Nyenswah, T. G., Ndeffo-Mbah, M. L., and Galvani, A. P., "Strategies for containing ebola in west africa," *Science*, vol. 346, no. 6212, pp. 991–995, 2014.

[27] Pastor-Satorras, R. and Vespignani, A., "Epidemic spreading in scale-free networks," *Phys. Rev. Lett.*, vol. 86, pp. 3200–3203, Apr 2001.

[28] Perra, N., Balcan, D., Gonalves, B., and Vespignani, A., "Towards a characterization of behavior-disease models," *PLoS ONE*, vol. 6, 08 2011.

[29] Preciado, V. M., Sahneh, F. D., and Scoglio, C., "A convex framework for optimal investment on disease awareness in social networks," in *Global Conference on Signal and Information Processing (GlobalSIP), 2013 IEEE*, pp. 851–854, Dec 2013.

[30] Preciado, V., Zargham, M., Enyioha, C., Jadbabaie, A., and Pappas, G., "Optimal resource allocation for network protection against spreading processes," *Control of Network Systems, IEEE Transactions on*, vol. 1, pp. 99–108, March 2014.

[31] Reluga, T. C., "Game theory of social distancing in response to an epidemic," *PLoS Comput Biol*, vol. 6, p. e1000793, 05 2010.

[32] Rizzo, A., Frasca, M., and Porfiri, M., "Effect of individual behavior on epidemic spreading in activity-driven networks," *Phys. Rev. E*, vol. 90, p. 042801, Oct 2014.

[33] Ruhi, N. A. and Hassibi, B., "SIRS epidemics on complex networks: Concurrence of exact markov chain and approximated models," *CoRR*, vol. abs/1503.07576, 2015.

[34] SteelFisher, G. K., Blendon, R. J., Bekheit, M. M., and Lubell, K., "The public's response to the 2009 h1n1 influenza pandemic," *New England Journal of Medicine*, vol. 362, no. 22, p. e65, 2010. PMID: 20484390.

[35] Trajanovski, S., Hayel, Y., Altman, E., Wang, H., and Van Mieghem, P., "Decentralized protection strategies against sis epidemics in networks," *Control of Network Systems, IEEE Transactions on*, vol. 2, pp. 406–419, Dec 2015.

[36] Van De Bovenkamp, R. and Van Mieghem, P., "Time to metastable state in sis epidemics on graphs," in *Signal-Image Technology and Internet-Based Systems (SITIS), 2014 Tenth International Conference on*, pp. 347–354, Nov 2014.

[37] Van Mieghem, P., Omic, J., and Kooij, R., "Virus spread in networks," *Networking, IEEE/ACM Transactions on*, vol. 17, pp. 1–14, Feb 2009.

[38] Volz, E. M., Miller, J. C., Galvani, A., and Ancel Meyers, L., "Effects of heterogeneous and clustered contact patterns on infectious disease dynamics," *PLoS Comput Biol*, vol. 7, p. e1002042, 06 2011.

[39] Wang, Y., Chakrabarti, D., Wang, C., and Faloutsos, C., "Epidemic spreading in real networks: an eigenvalue viewpoint," in *Reliable Distributed Systems, 2003. Proceedings. 22nd International Symposium on*, pp. 25–34, Oct 2003.

[40] Wang, Z., Andrews, M. A., Wu, Z.-X., Wang, L., and Bauch, C. T., "Coupled diseasebehavior dynamics on complex networks: A review," *Physics of Life Reviews*, vol. 15, pp. 1 – 29, 2015.

[41] Watts, D. J. and Strogatz, S. H., "Collective dynamics of'small-world'networks.," *Nature*, vol. 393, no. 6684, pp. 409–10, 1998.

[42] Wu, Q., Fu, X., Small, M., and Xu, X.-J., "The impact of awareness on epidemic spreading in networks," *Chaos*, vol. 22, no. 1, 2012.

[43] Zhang, H.-F., Xie, J.-R., Tang, M., and Lai, Y.-C., "Suppression of epidemic spreading in complex networks by local information based behavioral responses," *Chaos*, vol. 24, no. 4, 2014.

[44] Zhang, J. and Moura, J., "Diffusion in social networks as sis epidemics: Beyond full mixing and complete graphs," *Selected Topics in Signal Processing, IEEE Journal of*, vol. 8, pp. 537–551, Aug 2014.